Increased *Col10a1* expression is not causative for the phenotype of Phex-deficient *Hyp* mice

Timur Yorgan [a,1], Carsten Rendenbach [a,1], Anke Jeschke [a,1], Michael Amling [a],
Kathryn S.E. Cheah [b], Thorsten Schinke [a,*]

[a] *Department of Osteology and Biomechanics, University Medical Center Hamburg Eppendorf, Hamburg, Germany*
[b] *Department of Biochemistry, University of Hongkong, Hongkong, China*

ABSTRACT

X-linked hypophosphatemic rickets (XLHR) is a severe disorder of phosphate homeostasis and skeletal mineralization caused by mutations of *PHEX*, encoding a bone-specific endopeptidase. Phex-deficient *Hyp* mice have been extensively studied to understand the molecular bases of XLHR, and here it was found that *Fgf23*, encoding a major phosphaturic hormone, was transcriptionally activated in bone-forming osteoblasts. We and others could additionally show that *Col10a1* expression is increased in *Hyp* osteoblasts and bones, thereby raising the possibility that ectopic production of type X collagen could contribute to the impaired mineralization of the *Hyp* bone matrix. Here we show that an additional deficiency of the *Col10a1* gene does not overtly affect the skeletal phenotype of *Hyp* mice. More specifically, *Col10a1*-deficient *Hyp* mice displayed severe disturbances of skeletal growth, bone mass acquisition and bone matrix mineralization, and they were essentially indistinguishable from *Hyp* littermates. This was confirmed by non-decalcified histology and bone-specific histomorphometry quantifying all relevant parameters of growth plate maturation, trabecular bone architecture and osteoid accumulation. Taken together, our results show that increased *Col10a1* expression in Phex-deficient osteoblasts is not a major cause of the XLHR phenotype, which was an important issue to address based on the previous findings.

© 2013 Elsevier Inc. All rights reserved.

1. Introduction

Phosphate homeostasis is tightly linked to skeletal mineralization, not only because low serum phosphate concentrations (hypophosphatemia) can result in decreased bone matrix mineralization (osteomalacia), but also because the most critical regulators of renal phosphate handling are expressed in bone [1]. More specifically, there is hallmark genetic evidence, that Fgf23 is the most relevant regulator of phosphate homeostasis in mice and humans [2]. Of note, Fgf23 is predominantly expressed by matrix-embedded terminally differentiated osteoblasts (osteocytes) and it primarily acts in the kidney, where it regulates the expression of at least three relevant target genes, *Slc34a1* (encoding a sodium-phosphate cotransporter), as well as *Cyp27b1* and *Cyp24a1* (encoding hydroxylases activating or inactivating vitamin D) [3]. The key role of Fgf23 in phosphate homeostasis is underscored by the fact that activating *FGF23* mutations cause autosomal dominant hypophosphatemic rickets, whereas inactivating *FGF23* mutations cause

an autosomal recessive hyperphosphatemic disorder known as tumoral calcinosis [4,5]. Importantly, high circulating FGF23 levels are also found in other genetic and acquired disorders of renal phosphate loss, such as autosomal recessive and X-linked hypophosphatemic rickets, as well as tumor-induced osteomalacia [2,6].

The most common form of inherited hypophosphatemic rickets, with an incidence of 1 in 20,000 newborns, is XLHR, where the underlying genetic defect was identified in 1995 [7]. The affected gene was termed *PHEX* (Phosphate-regulating gene with homologies to endopeptidases on the X-chromosome), and since a mouse model (termed *Hyp*) with a spontaneous deletion within the murine *Phex* gene was already available, it was possible to obtain some important insights into the pathophysiology of XLHR [8]. More specifically it was found that the hypophosphatemia in *Hyp* mice is caused by a circulating phosphaturic factor, later identified as Fgf23, and not by an intrinsic renal defect [9–11]. Likewise, Phex is not expressed in the kidney, but by terminally differentiated osteoblasts, also known as the main producers of Fgf23 [12,13]. The severe impairment of skeletal mineralization in *Hyp* mice is partially explained by their hypophosphatemia, yet there is steadily increasing evidence for a cell-autonomous defect of Phex-deficient osteoblasts and an Fgf23-independent role of Phex in skeletal mineralization [14–19]. Since the Phex protein shares

homologies to a family of endopeptidases it has been speculated that Phex acts by cleaving specific substrates that could act downstream of Phex to control serum phosphate levels and/or bone mineralization [20]. Importantly however, Fgf23 is not cleaved and thereby inactivated by Phex, unlike it was initially hypothesized [20,21]. Instead, *Fgf23* was found transcriptionally activated in Phex-deficient bone cells, thus implying that the XLHR pathologies are related to changes in gene expression [22,23].

In this regard it is important to state that two studies have been performed to analyze the impact of Phex-deficiency on gene expression in an unbiased approach. First, RNA was isolated from long bones of wildtype and *Hyp* mice and subjected to genome-wide expression analysis [23]. Here it was found that three genes were expressed at more than 5-fold higher rate in *Hyp* mice, namely *Fgf23*, *Thbs4* and *Col10a1*. Second, we have previously applied genome-wide expression analysis to compare primary calvarial osteoblasts from wildtype and *Hyp* mice at day 25 of differentiation [19]. Here we identified four genes with more than 5-fold higher expression in *Hyp* osteoblasts, namely *Mlana*, *Aqp5*, *Fgf23* and *Col10a1*. Regardless of the potential limitations associated with global expression analyses, it was remarkable that both studies identified *Fgf23* and *Col10a1* as Phex-regulated genes, and while the contribution of Fgf23 to the XLHR pathology has already been proven, it was quite important to address the relevance of *Col10a1* induction as well. More specifically, our hypothesis was that the ectopic presence of type X collagen, endoded by the *Col10a1* gene, in the bone matrix would interfere with the mineralization process and thereby explain, at least in part, the osteomalacia phenotype of *Hyp* mice. Moreover, since *Hyp* mice additionally display hypomineralization of growth plate cartilage with persistence of cartilage remnants in the primary spongiosa [24], it remained to be established, if increased type X collagen production by hypertrophic chondrocytes would contribute to the growth defects of *Hyp* mice. For that purpose we generated *Col10a1*-deficient *Hyp* mice and analyzed their skeletal phenotype.

2. Materials and methods

2.1. Animals

Hyp mice (C57Bl/6 genetic background) were obtained from the Jackson Laboratory (#000528), while *Col10a1*-deficient mice were described previously [25]. Genotypes were determined by genomic PCR with the following primer combinations. While the presence of the *Phex* exon 21 was detected using 5′-CGA CCA GGA TGA GGG AAG AAA G -3′ and 5′-CAC TTG TTC TCT GGC AGC TTC TG-3′ (486 bp product), the *Hyp* mutation was detected by 5′-CAG GGG ACT GTC CAC AAG GGG G-3′ and 5′-GGG TGC AAA GGT GTT GTG AAT GGA A-3′ (669 bp product). For *Col10a1* genotyping we used 5′-ATA CCT TCT CGT CCT TGC TT-3′ and 5′-ACA CAA AGG AGA TAT TGG CC-3′ for the wildtype allele (417 bp product) and 5′-ATA CCT TCT CGT CCT TGC TT-3′ and 5′-AGG GGA GGA GTA GAA GGT GG-3′ for the mutant allele (535 bp product). All animal experiments were approved by the animal facility of the University Medical Center Hamburg-Eppendorf and by the ''Amt für Gesundheit und Verbraucherschutz'' (Org529).

2.2. Immunohistochemistry

Immunohistochemistry was performed on decalcified and paraffin-embedded tibia sections from wildtype and *Hyp* mice. For immunohistochemical detection sections were deparaffinized, rehydrated, and pre-treated for antigen unmasking with pepsin for type X collagen or 0.2% hyaluronic acid for type l collagen. To block endogenous peroxidase activity and non-specific antibody binding, sections were incubated with 3% hydrogen peroxide for 15 min and with 5% BSA for 30 min. Antibodies against type I collagen (1:600, Cedarlane) or type X collagen (1:20, Quartett) were applied over night at 4 °C. Biotinylated goat anti-rabbit IgG (1:200, Dako Cytomation) and rabbit anti-mouse IgG (1:200, Dako Cytomation) for 30 min were used as a secondary antibody, followed by incubation of 30 min with streptavidin/HRP (1:200, Dako Cytomation). Peroxidase activity was detected using DAB as a chromogenic substrate (Dako Cytomation). Sections were counterstained with hematoxylin/eosin, dehydrated, and mounted.

2.3. Skeletal analysis

After their initial analysis by contact X-ray (Faxitron X-ray Corp.), the vertebral bodies L2 to L5 and one tibia from each animal were dehydrated and embedded non-decalcified into methylmetacrylate for sectioning. A fixed-blade rotation microtome was used to cut 4 μm thick sections. These sections were either stained with toluidine blue or by the von Kossa/van Gieson procedure as described [26]. In brief, for toluidine blue staining the sections were incubated for 30 min at ambient temperature in 1% toluidine blue solution (pH 4.5). The Kossa/van Gieson staining was achieved by initially incubating the sections in 3% silver nitrate for 5 min followed by additional 5 min in 5% sodium thiosulfate. Van Gieson solution (0.25% acid fuchsine, 0.5% nitric acid, 10% glycerine, and picric acid to saturation) was used to counterstain the sections for 20 min. The resulting staining shows mineralized bone matrix in black and non-mineralized osteoid in red. Static histomorphometry was performed on Kossa/van Gieson stained sections using the Bioquant Osteo software (BIOQUANT Image Analysis Corporation, Nashville, USA). Additional histomorphometry for the analysis of osteoid parameters was carried out on toluidine blue-stained sections using the OsteoMeasure system (Osteometrics, Decatur, USA) following the guidelines of the American Society of Bone and Mineral Research [27].

2.4. Statistical analysis

All data are presented as means ± standard deviation. Statistical analysis was performed with Prism v6.01 (Graphpad Software, Inc., La Jolla, USA) using an one-way ANOVA followed post hoc by Turkey's range test for multiple comparisons. The *p*-value threshold for significance was set at 0.05.

3. Results

We first performed immunohistochemistry to address the question, if type X collagen is detectable in the bone matrix of Phex-deficient *Hyp* mice. When we analyzed tibia sections from 6 weeks old wildtype mice, we found intensive staining for type X collagen only in hypertrophic cartilage, as expected. In contrast, there was additional staining for type X collagen in the primary spongiosa of 6 weeks old *Hyp* mice, consistent with *Col10a1* over-expression (Fig. 1A). To analyze, whether this difference is attributable to the presence of cartilage remnants in the primary spongiosa of *Hyp* mice, we analyzed consecutive sections incubated with antibodies against type X collagen or type I collagen. Here we found that areas being positive for type X collagen appeared negative for type I collagen (Fig. 1B). Most importantly, the bone matrix stained with the antibody against type I collagen did not display an intense staining for type X collagen. Taken together, these results suggested that the primary spongiosa of *Hyp* mice contains a larger number of cartilage remnants compared to wildtype littermates, but that the bone matrix of *Hyp* mice does not contain the same amount of type X collagen compared to hypertrophic cartilage.
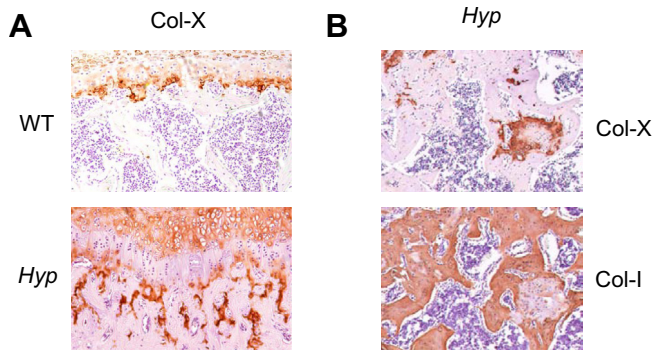
Fig. 1. Type X collagen distribution in *Hyp* bones. (A) Immunohistochemistry with antibodies against type X collagen (Col-X) on decalcified tibia sections from 6 weeks old wildtype (WT) and *Hyp* mice. (B) Immunohistochemistry with antibodies against type X collagen (Col-X) or type I collagen (Col-I) on consecutive decalcified tibia sections from *Hyp* mice. Note that Col-X-positive areas are negative for Col-I and vice versa.

Regardless of these initial findings we next addressed the question, whether a moderate ectopic production of type X collagen by *Hyp* osteoblasts contributes to the skeletal phenotype of *Hyp* mice. Therefore, we mated $Col10a1^{+/-}/Hyp^{+/0}$ males with $Col10a1^{+/-}/Hyp^{+/-}$ females and analyzed male littermates with the genotypes

$Col10a1^{+/+}/Hyp^{+/0}$, $Col10a1^{-/-}/Hyp^{+/0}$, $Col10a1^{+/+}/Hyp^{-/0}$ and $Col10a1^{-/-}/Hyp^{-/0}$ at 6 weeks of age. Using contact X-rays we observed that the severe skeletal phenotype of *Hyp* mice was not obviously influenced by additional *Col10a1* deficiency (Fig. 2A). Toluidine blue staining of the tibial growth plate further demonstrated that the severe disturbances of growth plate mineralization in *Hyp* mice were not affected by *Col10a1* deficiency (Fig. 2B). Moreover, when we quantified femur length, growth plate thickness and the number of rachitic cartilage remnants in all four groups of mice, there were statistically significant differences between $Hyp^{+/0}$ and $Hyp^{-/0}$ mice, but these were not significantly affected by *Col10a1* deficiency (Fig. 2C).

We next analyzed the bone phenotypes of $Col10a1^{+/+}/Hyp^{+/0}$, $Col10a1^{-/-}/Hyp^{+/0}$, $Col10a1^{+/+}/Hyp^{-/0}$ and $Col10a1^{-/-}/Hyp^{-/0}$ mice by histomorphometric analysis of spine sections (Fig. 3A). Similar to the findings on skeletal growth, we observed that the trabecular bone volume and trabecular number were significantly lower in $Hyp^{-/0}$ mice, but there was again no influence of the additional *Col10a1* deficiency (Fig. 3B).

The most important analysis related to our initial question was however a quantification of osteoid parameters in the four groups of mice, since the primary bone defect of *Hyp* mice is a severe enrichment of osteoid, representing non-mineralized bone matrix (Fig. 4A). Here we found, as expected, that osteoid volume per bone volume, osteoid surface per bone surface and osteoid thickness
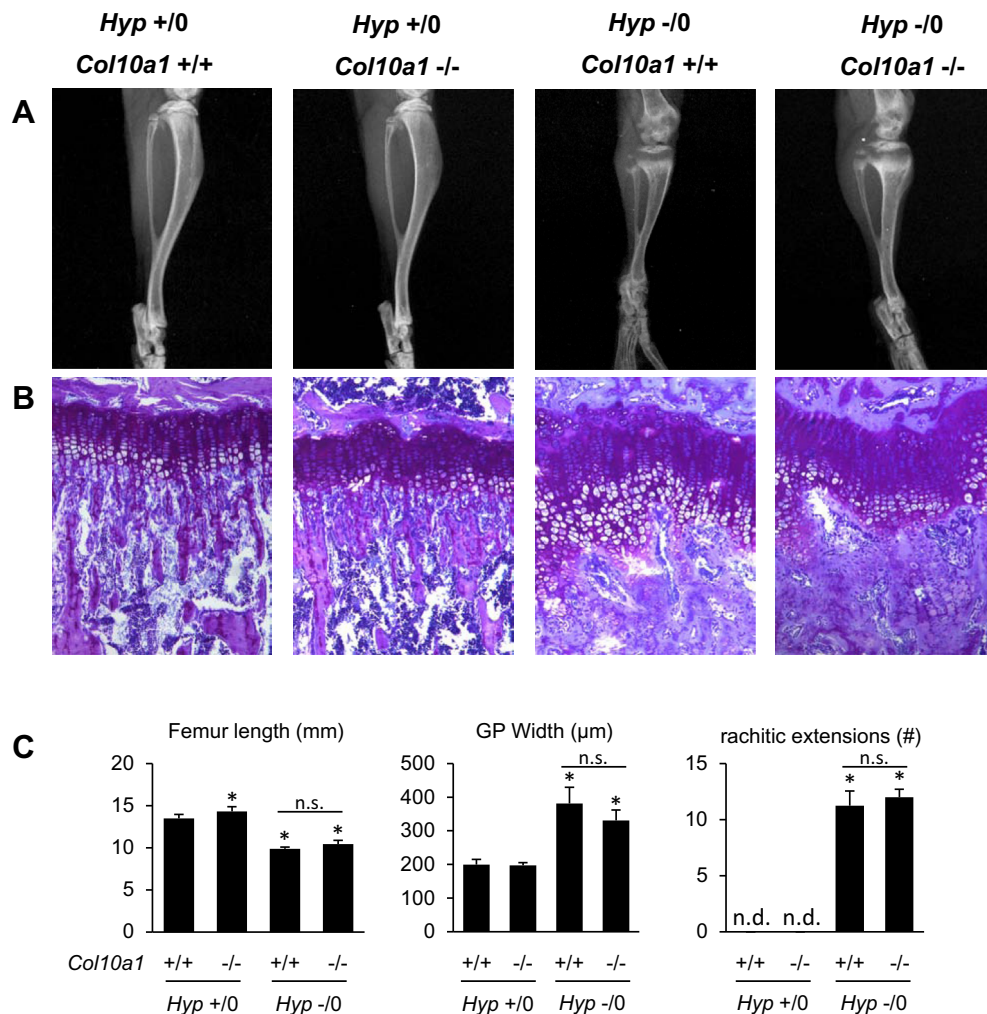

Fig. 2. Impaired skeletal growth in *Col10a1*-deficient *Hyp* mice. (A) Contact X-rays of the tibia from 6 weeks old mice of the indicated genotypes. (B) Toluidine blue staining of the tibial growth plate from the same mice. (C) Quantification of the femur length, the tibial growth plate thickness and the number of rachitic extensions of hypertrophic cartilage. Bars represent mean ± SD ($n = 5$ per group). Asterisks indicate statistically significant differences compared to wildtype mice ($p < 0.05$).
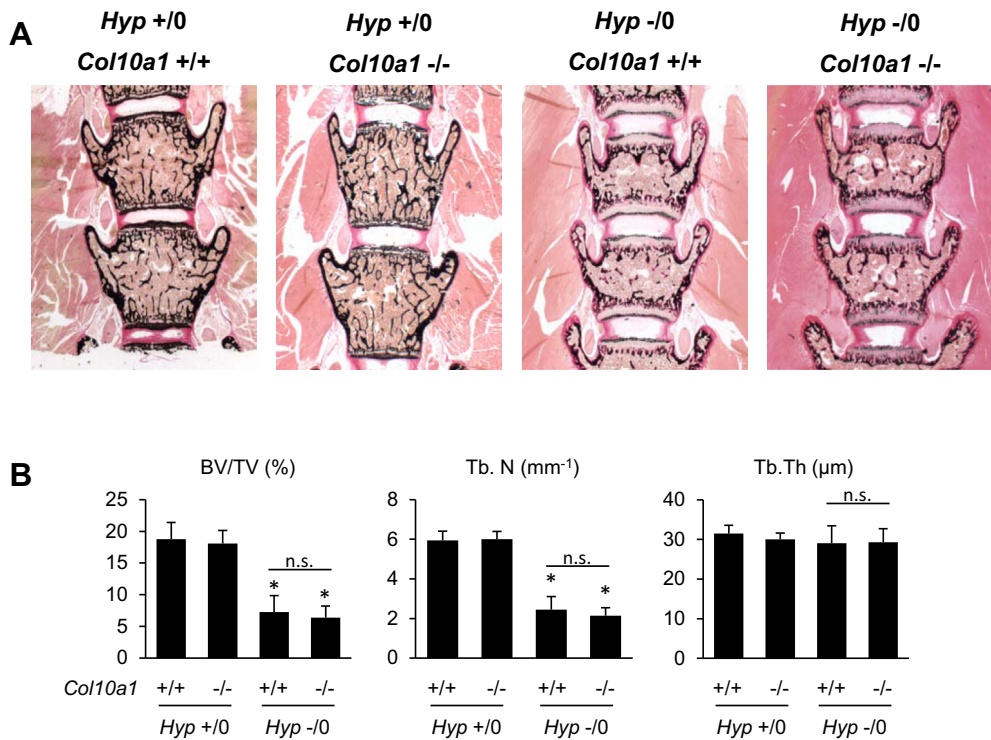
Fig. 3. Decreased bone mass in *Col10a1*-deficient *Hyp* mice. (A) Von Kossa/van Gieson staining of spine sections from 6 weeks old mice of the indicated genotypes. Mineralized bone matrix is stained black, while non-mineralized osteoid is stained red. (B) Histomorphometric quantification of the trabecular bone volume (BV/TV, bone volume per tissue volume), trabecular number (Tb.N.) and trabecular thickness (Tb.Th.). Bars represent mean ± SD ($n = 5$ per group). Asterisks indicate statistically significant differences compared to wildtype mice ($p < 0.05$). (For interpretation of the references to color in this figure legend, the reader is referred to the web version of this article.)
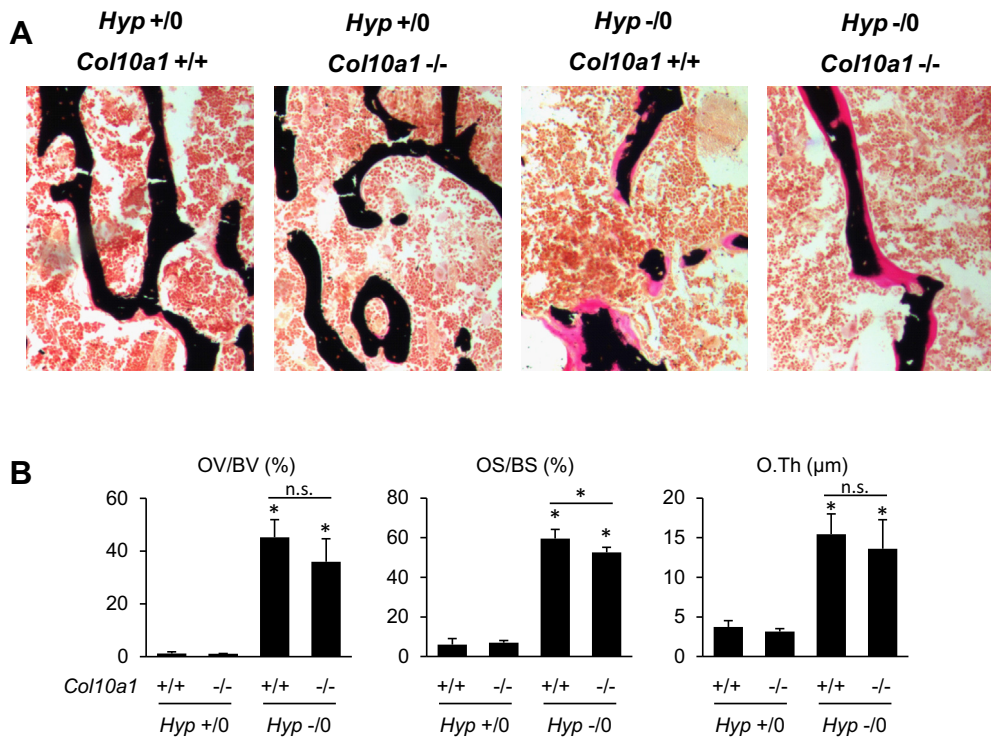

Fig. 4. Osteomalacia in *Col10a1*-deficient *Hyp* mice. (A) Von Kossa/van Gieson staining of spine sections from 6 weeks old mice of the indicated genotypes. High magnification images reveal enrichment of non-mineralized osteoid in *Hyp* mice. (B) Histomorphometric quantification of the osteoid volume (OV/BV, osteoid volume per bone volume), osteoid surface (OS/BS, osteoid surface per bone surface) and osteoid thickness (O.Th.). Bars represent mean ± SD ($n = 5$ per group). Asterisks directly above bars indicate statistically significant differences compared to wildtype mice ($p < 0.05$). Asterisks above horizontal lines indicate significant differences between the concerned groups ($p < 0.05$), otherwise they are marked n.s. for no significance.

were all markedly increased in $Hyp^{-/0}$ mice (Fig. 4B). The comparison of these parameters between $Col10a1^{+/+}/Hyp^{-/0}$ and $Col10a1^{-/-}/Hyp^{-/0}$ littermates revealed non-significant differences in terms of osteoid volume per bone volume and osteoid thickness, yet osteoid surface per bone surface was significantly reduced in $Col10a1^{-/-}/Hyp^{-/0}$ mice. Taken together, these data demonstrate that ectopic production of type X collagen by Phex-deficient osteoblasts has only a moderate influence on bone matrix mineralization, thus suggesting that it is not a major pathogenic factor in XLHR.

4. Discussion

Based on previously performed genome-wide expression analyses by us and by others, we hypothesized that increased Col10a1 expression by Phex-deficient bone cells would contribute to the skeletal abnormalities of Phex-deficient Hyp mice [19,23]. In support of this hypothesis, we have previously found that retinol deprivation partially corrects the osteomalacia of Hyp mice in a hypophosphatemia-independent manner [19]. Since Col10a1 has been identified as a retinoic acid-induced gene [28], and since retinol administration to Hyp osteoblasts further increased Col10a1 expression [19], it was reasonable to speculate that increased retinol responsiveness of Hyp osteoblasts contributes to the bone mineralization defects of Hyp mice through a Col10a1-dependent mechanism. Likewise, as type X collagen has been reported to inhibit mineralization processes in vitro [29], it appeared likely that its ectopic presence in the Hyp bone matrix could interfere with mineralization and cause osteomalacia. Most importantly however, it is still remarkable that the in vivo and ex vivo genome-wide expression analyses came up with only few genes being 5-fold over-expressed upon Phex-deficiency, and that the only two common genes were Fgf23 and Col10a1.

Based on these arguments it was highly important to address the role of Col10a1 in the context of XLHR, which we did by generating and analyzing Col10a1-deficient Hyp mice. Using a thorough skeletal phenotyping approach, including undecalcified histology and histomorphometry, we are now able to state that ectopic Col10a1 expression by Hyp osteoblasts is not causative for the osteomalacia of Hyp mice. It is further questionable that this ectopic expression results in significant enrichment of type X collagen in the bone matrix, since our immunohistochemistry revealed that the majority of type X collagen enrichment in Hyp mice is explained by the presence of cartilage remnants. While these findings do not rule out that type X collagen is present in the Hyp bone matrix at lower levels than in hypertrophic cartilage we can certainly rule out a significant impact of ectopic Col10a1 expression on the Hyp phenotype.

In summary, our study provides a negative result and a falsification of our initial hypothesis. Nevertheless, given the striking overlap of two unbiased gene expression studies with respect to Col10a1, it was extremely important to perform these analyses, especially since the key role of Phex in skeletal mineralization is still poorly to be understood at the molecular level [30].

References

[1] M. Christov, H. Juppner, Insights from genetic disorders of phosphate homeostasis, Semin. Nephrol. 33 (2013) 143–157.

[2] C. Bergwitz, H. Juppner, FGF23 and syndromes of abnormal renal phosphate handling, Adv. Exp. Med. Biol. 728 (2012) 41–64.

[3] T. Shimada, H. Hasegawa, Y. Yamazaki, T. Muto, R. Hino, Y. Takeuchi, T. Fujita, K. Nakahara, S. Fukumoto, T. Yamashita, FGF-23 is a potent regulator of vitamin D metabolism and phosphate homeostasis, J. Bone Miner. Res. 19 (2004) 429–435.

[4] T.A. Consortium, Autosomal dominant hypophosphataemic rickets is associated with mutations in FGF23, Nat. Genet. 26 (2000) 345–348.

[5] A. Benet-Pages, P. Orlik, T.M. Strom, B. Lorenz-Depiereux, An FGF23 missense mutation causes familial tumoral calcinosis with hyperphosphatemia, Hum. Mol. Genet. 14 (2005) 385–390.

[6] W.H. Chong, A.A. Molinolo, C.C. Chen, M.T. Collins, Tumor-induced osteomalacia, Endocr. Relat. Cancer 18 (2011) R53–R77.

[7] T.H. Consortium, A gene (PEX) with homologies to endopeptidases is mutated in patients with X-linked hypophosphatemic rickets. The HYP Consortium, Nat. Genet. 11 (1995) 130–136.

[8] T.M. Strom, F. Francis, B. Lorenz, A. Boddrich, M.J. Econs, H. Lehrach, T. Meitinger, Pex gene deletions in Gy and Hyp mice provide mouse models for X-linked hypophosphatemia, Hum. Mol. Genet. 6 (1997) 165–171.

[9] R.A. Meyer Jr., M.H. Meyer, R.W. Gray, Parabiosis suggests a humoral factor is involved in X-linked hypophosphatemia in mice, J. Bone Miner. Res. 4 (1989) 493–500.

[10] T. Nesbitt, T.M. Coffman, R. Griffiths, M.K. Drezner, Crosstransplantation of kidneys in normal and Hyp mice, Evidence that the Hyp mouse phenotype is unrelated to an intrinsic renal defect, J Clin Invest 89 (1992) 1453–1459.

[11] H.S. Tenenhouse, L. Beck, Renal Na(+)-phosphate cotransporter gene expression in X-linked Hyp and Gy mice, Kidney Int. 49 (1996) 1027–1032.

[12] L. Du, M. Desbarats, S. Cornibert, D. Malo, B. Ecarot, Fine genetic mapping of the Hyp mutation on mouse chromosome X, Genomics 32 (1996) 177–183.

[13] R. Guo, L.D. Quarles, Cloning and sequencing of human PEX from a bone cDNA library: evidence for its developmental stage-specific regulation in osteoblasts, J. Bone Miner. Res. 12 (1997) 1009–1017.

[14] B. Ecarot, F.H. Glorieux, M. Desbarats, R. Travers, L. Labelle, Defective bone formation by Hyp mouse bone cells transplanted into normal mice. evidence in favor of an intrinsic osteoblast defect, J. Bone Miner. Res. 7 (1992) 215–220.

[15] M. Murshed, D. Harmey, J.L. Millan, M.D. McKee, G. Karsenty, Unique coexpression in osteoblasts of broadly expressed genes accounts for the spatial restriction of ECM mineralization to bone, Genes Dev. 19 (2005) 1093–1104.

[16] B. Ecarot, F.H. Glorieux, M. Desbarats, R. Travers, L. Labelle, Effect of dietary phosphate deprivation and supplementation of recipient mice on bone formation by transplanted cells from normal and X-linked hypophosphatemic mice, J. Bone Miner. Res. 7 (1992) 523–530.

[17] S. Liu, W. Tang, J. Zhou, L. Vierthaler, L.D. Quarles, Distinct roles for intrinsic osteocyte abnormalities and systemic factors in regulation of FGF23 and bone mineralization in Hyp mice, Am. J. Physiol. Endocrinol. Metab. 293 (2007) E1636–E1644.

[18] Z.S. Xiao, M. Crenshaw, R. Guo, T. Nesbitt, M.K. Drezner, L.D. Quarles, Intrinsic mineralization defect in Hyp mouse osteoblasts, Am. J. Physiol. 275 (1998) E700–E708.

[19] S. Seitz, C. Rendenbach, F. Barvencik, T. Streichert, A. Jeschke, J. Schulze, M. Amling, T. Schinke, Retinol deprivation partially rescues the skeletal mineralization defects of Phex-deficient Hyp mice, Bone 53 (2013) 231–238.

[20] R. Guo, S. Liu, R.F. Spurney, L.D. Quarles, Analysis of recombinant Phex: an endopeptidase in search of a substrate, Am. J. Physiol. Endocrinol. Metab. 281 (2001) E837–E847.

[21] A. Benet-Pages, B. Lorenz-Depiereux, H. Zischka, K.E. White, M.J. Econs, T.M. Strom, FGF23 is processed by proprotein convertases but not by PHEX, Bone 35 (2004) 455–462.

[22] S. Liu, R. Guo, L.G. Simpson, Z.S. Xiao, C.E. Burnham, L.D. Quarles, Regulation of fibroblastic growth factor 23 expression but not degradation by PHEX, J. Biol. Chem. 278 (2003) 37419–37426.

[23] S. Liu, W. Tang, J. Fang, J. Ren, H. Li, Z. Xiao, L.D. Quarles, Novel regulators of Fgf23 expression and mineralization in Hyp bone, Mol. Endocrinol. 23 (2009) 1505–1518.

[24] D. Miao, X. Bai, D.K. Panda, A.C. Karaplis, D. Goltzman, M.D. McKee, Cartilage abnormalities are associated with abnormal Phex expression and with altered matrix protein and MMP-9 localization in Hyp mice, Bone 34 (2004) 638–647.

[25] K.M. Kwan, M.K. Pang, S. Zhou, S.K. Cowan, R.Y. Kong, T. Pfordte, B.R. Olsen, D.O. Sillence, P.P. Tam, K.S. Cheah, Abnormal compartmentalization of cartilage matrix components in mice lacking collagen X: implications for function, J. Cell Biol. 136 (1997) 459–471.

[26] J. Albers, J. Keller, A. Baranowsky, F.T. Beil, P. Catala-Lehnen, J. Schulze, M. Amling, T. Schinke, Canonical Wnt signaling inhibits osteoclastogenesis independent of osteoprotegerin, J. Cell Biol. 200 (2013) 537–549.

[27] A.M. Parfitt, M.K. Drezner, F.H. Glorieux, J.A. Kanis, H. Malluche, P.J. Meunier, S.M. Ott, R.R. Recker, Bone histomorphometry: standardization of nomenclature, symbols, and units. Report of the ASBMR Histomorphometry Nomenclature Committee, J. Bone Miner. Res. 2 (1987) 595–610.

[28] A.J. Cohen, L. Lassova, E.B. Golden, Z. Niu, S.L. Adams, Retinoids directly activate the collagen X promoter in prehypertrophic chondrocytes through a distal retinoic acid response element, J. Cell Biochem. 99 (2006) 269–278.

[29] J.L. Arias, O. Nakamura, M.S. Fernandez, J.J. Wu, P. Knigge, D.R. Eyre, A.I. Caplan, Role of type X collagen on experimental mineralization of eggshell membranes, Connect Tissue Res. 36 (1997) 21–33.

[30] P.S. Rowe, Regulation of bone-renal mineral and energy metabolism: the PHEX, FGF23, DMP1, MEPE ASARM pathway, Crit. Rev. Eukaryot. Gene Expr. 22 (2012) 61–86.